HHS Public Access

Author manuscript

Nat Chem Biol. Author manuscript; available in PMC 2016 January 01.

Published in final edited form as:

Nat Chem Biol. 2015 July ; 11(7): 504–510. doi:10.1038/nchembio.1814.

Convergence of Biological Nitration and Nitrosation via Symmetrical Nitrous Anhydride

Dario A. Vitturi[1], **Lucia Minarrieta**[2], **Sonia R. Salvatore**[1], **Edward M. Postlethwait**[3], **Marco Fazzari**[1,4], **Gerardo Ferrer-Sueta**[5,6], **Jack R. Lancaster Jr.**[1,7,8], **Bruce A. Freeman**[1,#], and **Francisco J. Schopfer**[1,#]

[1]Department of Pharmacology and Chemical Biology, University of Pittsburgh. Pittsburgh, PA, USA.

[2]Cátedra de Inmunología, Universidad de la República, Montevideo, Uruguay.

[3]Department of Environmental Health Sciences, University of Alabama at Birmingham, Birmingham, AL, USA.

[4]Fondazione Ri.MED, Palermo, Italy.

[5] Laboratorio de Fisicoquímica Biológica, Universidad de la República, Montevideo, Uruguay.

[6]Center for Free Radical and Biomedical Research. Universidad de la República, Montevideo, Uruguay.

[7]Department of Medicine University of Pittsburgh. Pittsburgh, PA, USA.

[8]Department of Surgery. University of Pittsburgh. Pittsburgh, PA, USA.

Abstract

Current perspective holds that the generation of secondary signaling mediators from nitrite (NO_2^-) requires acidification to nitrous acid (HNO_2) or metal catalysis. Herein, the use of stable isotope-labeled NO_2^- and LC-MS/MS analysis of products revealed that NO_2^- also participates in fatty acid nitration and thiol S-nitrosation at neutral pH. These reactions occur in the absence of metal centers and are stimulated by nitric oxide ($^{\bullet}NO$) autoxidation via symmetrical dinitrogen trioxide (nitrous anhydride, $symN_2O_3$) formation. While theoretical models have predicted physiological $symN_2O_3$ formation, its generation is now demonstrated in aqueous reaction systems, cell models and *in vivo*, with the concerted reactions of $^{\bullet}NO$ and NO_2^- shown to be critical for $symN_2O_3$ formation. These results reveal new mechanisms underlying the NO_2^- propagation of $^{\bullet}NO$

[#]To whom correspondence may be addressed: Bruce A. Freeman, Ph.D. or Francisco J. Schopfer, Ph.D., Department of Pharmacology & Chemical Biology, Thomas E. Starzl Biomedical Science Tower E1340, 200 Lothrop St, University of Pittsburgh, Pittsburgh, PA 15213, USA; Tel: 648-9319; Fax: (412) 648-2229; freerad@pitt.edu or fjs2@pitt.edu..

Author contributions: DAV designed, performed and analyzed experiments, as well as wrote the manuscript. LM designed, performed and analyzed cell-based experiments. SRS performed high resolution LC-MS/MS experiments and contributed to overall LC-MS/MS method development. EMP designed and performed $^{\bullet}NO_2$ gas experiments. MF developed extraction methods for *in vivo* experiments. GFS contributed to data interpretation. JRL designed experiments, contributed to data interpretation and provided critical insight into manuscript content. BAF contributed to the overall concept, experimental design and manuscript preparation. FJS designed experiments, contributed to data analysis and interpretation as well as manuscript writing.

Competing Financial Interests Statement: BAF and FJS acknowledge financial interest in Complexa, Inc.

signaling and the regulation of both biomolecule function and signaling network activity via NO_2^--dependent nitrosation and nitration reactions.

The signaling responses and chemical reactions induced by nitric oxide (•NO) during both physiological and metabolically-stressed conditions affirm that, in addition to the activation of guanylate cyclase-dependent cGMP production, non cGMP-dependent reactions contribute to •NO regulation of biomolecule structure and function. In this regard, the S-nitrosation of protein thiols by •NO can modulate protein function and downstream metabolic responses including vascular homeostasis, ion transport, cytoskeletal function and mitochondrial respiration [1]. The mechanisms responsible for S-nitrosothiol formation remain controversial and can include membrane-catalyzed •NO autoxidation, •NO reaction with heme centers, formation of dinitrosyl iron complexes, •NO reaction with thiyl radicals and thiols followed by one-electron oxidation, and thiol reaction with dinitrogen trioxide (nitrous anhydride, N_2O_3) [2-6]. The biological relevance of S-nitrosothiol formation in general, and S-nitrosoglutathione (GSNO) in particular, is supported by studies showing that alterations in the activity of a class III alcohol dehydrogenase, an enzyme that also metabolizes nitrosothiols, modulates the nitrosothiol proteome and physiological responses of murine models [7,8].

Many of the reactions that yield nitrosating intermediates also produce the nitrating species nitrogen dioxide ($^\bullet NO_2$). The nitration of protein tyrosine and tryptophan residues by $^\bullet NO_2$ may influence signaling networks but, unlike S-nitrosation, protein nitration is an irreversible and typically toxic post-translational protein modification (PTM) that occurs in concert with additional amino acid oxidation reactions [9]. In contrast, unsaturated fatty acids and guanine nucleotides are also nitrated by $^\bullet NO_2$ to yield electrophilic nitroalkene derivatives that react with nucleophilic cysteine and histidine residues of proteins. *In vitro* and *in vivo* studies support that the patterns of PTMs induced by “soft” nitroalkene electrophiles are not toxic and serve to link enzyme and transcriptional regulatory protein function with metabolic and inflammatory status [10-12]. For example, conjugated linoleic acid (CLA) is a physiological target of nitration, giving rise to nitro-conjugated linoleic acid (NO_2-CLA) regioisomers that are detectable in the urine and plasma of healthy humans at nM concentrations [13,14]. The levels of cell and tissue nitroalkenes are modulated by diet and oxidative inflammatory reactions involving •NO or nitrite (NO_2^-) [13,15,16].

Besides its dietary origin, NO_2^- is also a product of •NO autoxidation (reactions 1-4). In fact, •NO autoxidation is typically monitored by either measuring NO_2^- formation or the oxidation of fluorescent and chromogenic probes [4,17,18].

$$^\bullet NO + O_2 \rightleftarrows ONOO^\bullet + {}^\bullet NO \rightleftarrows N_2O_4 \quad (1)$$

$$N_2O_4 \rightleftarrows 2 \; {}^\bullet NO_2 \quad (2)$$

$$^\bullet NO_2 + {}^\bullet NO \rightleftarrows N_2O_3 \quad (3)$$

$$N_2O_3 + H_2O \rightleftarrows 2NO_2^- + 2H^+ \quad (4)$$

While these techniques accurately reflect reaction kinetics, none are capable of assessing whether NO_2^- reacts with nitrogen oxides derived from •NO autoxidation. Herein, isotopic labeling and LC/MS-MS analyses showed that both in chemical reaction systems and activated macrophages, ^{15}N-nitrite ($^{15}NO_2^-$) reacts with species generated during •NO autoxidation at physiological pH to yield the unsaturated fatty acid nitration product $^{15}NO_2$-CLA. Furthermore, we demonstrated that $^{15}NO_2^-$ also promotes GSH nitrosation, yielding ^{15}N-labeled GSNO (GS^{15}NO). These observations motivated additional study, as current paradigms hold that either an acidic environment capable of protonation of NO_2^- to HNO_2 (pK_a 3.46) or electron transfer reactions between NO_2^- $_2$and metal centers are required for the generation of secondary reactive species from NO_2^-. More specifically, HNO_2 dismutation yields •NO plus •NO_2 and, depending on their redox potential, metal centers can either oxidize NO_2^- to •NO_2 or catalyze the formation of •NO and N_2O_3 via NO_2^- reduction or reductive nitrosylation [16,19-21]. The observations reported herein are unprecedented, in that we showed that NO_2^- participates in concerted nitration and nitrosation reactions at neutral pH in the absence of metal catalysis. We demonstrated that these reactions are stimulated by •NO autoxidation via the formation of the symmetrical isomer of N_2O_3 (ONONO, symN_2O_3). Additionally, by using both cell-based and murine models of inflammation, we provide evidence that symN_2O_3 is a physiologically-relevant signaling intermediate.

RESULTS

•NO mediates NO_2^--dependent CLA nitration by macrophages

Conjugated linoleic acid is a preferential substrate for nitration in mice and in humans during both inflammatory conditions and digestive acidification. This is due to the unique reactivity of •NO_2 with the external flanking carbons of the conjugated diene moiety, which is more reactive than bis-allylic fatty acids by a factor of 10^4–10^5 [13]. Activation of the murine macrophage-like cell line RAW 264.7 induced CLA nitration (Figure 1a). The addition of $^{15}NO_2^-$ led to a dose-dependent increase in $^{15}NO_2$-CLA and a concomitant decrease in 14NO2-CLA, indicating that NO_2^- is a significant source of $^{\bullet NO}{}_2$ and that there is a competition between •NO-derived •$^{14}NO_2$ and $^{15}NO_2^-$-derived •$^{15}NO_2$ for CLA nitration. In these experiments, endogenous ^{14}•NO was the only source of both ^{14}•NO_2 and $^{14}NO_2^-$. Inhibition of inducible nitric oxide synthase (iNOS) generation of •NO with 1400W abrogated both $^{14}NO_2$-CLA and $^{15}NO_2$-CLA formation, which was restored by the addition of the •NO donor deta-NONOate (Figure 1b-c). This indicated that •NO is required for cellular NO_2^--dependent CLA nitration.

CLA nitration by •NO and NO_2^- does not require cells

The oxidation of NO to •$_2$ NO_2 *in vivo* is typically viewed to be catalyzed by metal centers (e.g., ferryl-heme complexes) or low pH conditions, with neither reaction including a role for •NO [20,22,23]. We next evaluated whether other cellular components, beyond iNOS-derived •NO, were required for NO_2^--mediated CLA nitration. Incubation of CLA with

the •NO-donor mahma-NONOate (MNO) in the absence of cells gave significant extents of $^{14}NO_2$-CLA formation (Figure 2a), consistent with $•NO_2$ generation from the reaction between •NO and dissolved O_2 [17]. Analogous to data in Figure 1a, addition of $^{15}NO_2^-$ dose-dependently decreased extents of $^{14}NO_2$-CLA formation and increased $^{15}NO_2$-CLA generation (Figure 2b-f). No CLA nitration occurred in the absence of •NO or when an aerobically-decayed •NO donor was added as a control, supporting that $•NO_2$ generation via HNO_2 disproportionation was negligible under these conditions (Figure 2g and Supplementary Results, Supplementary Fig. 1a). Similarly, we confirmed the absence of adventitious metal catalysis by treating our buffers with two different chelation strategies without affecting the yields of CLA nitration (Supplementary Figure 2). Although the individual rates of $^{14}NO_2$-CLA and $^{15}NO_2$-CLA formation were inversely modulated by $^{15}NO_2^-$ (Supplementary Fig. 3a), the global rate and the total yield of NO_2-CLA formation were only marginally affected (Figure 2g and Supplementary Fig. 3b).

Nitrite participates in •NO-dependent S-nitrosation

Nitric oxide autoxidation yields $•NO_2$ which, in the presence of •NO, supports the generation of N_2O_3. Within this context, thiol nitrosation occurs either by direct reaction with N_2O_3 or via $•NO_2$-dependent thiyl radical formation, followed by addition of •NO [17,24]. Addition of $^{15}NO_2^-$ to a system consisting of •NO, O_2 and GSH not only supported the formation of $GS^{14}NO$, but also dose-dependently yielded $GS^{15}NO$ (Figure 3a-f). No thiol nitrosation occurred in the absence of •NO, again ruling out HNO_2 formation and dismutation in thiol nitrosation (Figures 3g and Supplementary Fig. 1b). Similar to CLA nitration, $^{15}NO_2^-$ addition led to a dose-dependent increase in $GS^{15}NO$, with no effect on net nitrosothiol yield (Figure 3g and Supplementary Fig. 4a-c). While NO_2^- nitrosates thiols and amines under acidic conditions, NO_2^--dependent nitrosation reactions at neutral pH have only been previously detected upon metal center catalysis that often requires hypoxic conditions [23,25-27].

•NO_2 is needed for NO_2^--mediated nitration and nitrosation

Decreasing O_2 concentration ($pO_2 \leq 10$mmHg) and addition of the $•NO_2$ scavenger potassium ferrocyanide ($K_4Fe(CN)_6$, $k = 2\times10^6$ $M^{-1}s^{-1}$ [17]) inhibited both $^{14}NO_2$-CLA and $^{15}NO_2$-CLA production (Supplementary Fig. 5a-b). Similarly, these same conditions also inhibited the formation of $GS^{14}NO$ and $GS^{15}NO$ (Supplementary Fig. 5c-d), supporting a role for $•NO_2$ in NO_2^--dependent nitration and nitrosation reactions during •NO autoxidation.

Double isotope labeling reveals scrambling of NO_2^- atoms

The observation that ^{15}N from $^{15}NO_2^-$ was incorporated into both NO_2-CLA and GSNO suggested that $^{15}NO_2^-$ is oxidized by one electron to $^{15}•NO_2$ during •NO autoxidation and that $^{15}NO_2^-$ also supports the formation of ^{15}N-containing nitrosating species. These observations motivated the hypothesis that $^{15}NO_2^-$ reacts with •NO-derived nitrogen oxides to yield $symN_2O_3$ (**2**, Figure 4a). Unlike the asymmetrical isomer ($asymN_2O_3$, **1,** Figure 4a), the nitrogen atoms in $symN_2O_3$ are bonded to a central oxygen via two equivalent bonds that will homolyze with identical probability. Alternative homolysis of these N-O bonds

in ^{14}•NO/$^{15}NO_2^-$-derived symN_2O_3 would yield either ^{15}•NO_2 or ^{15}•NO (**2b** and **2d**, Figure 4a), thus providing a mechanism for explaining the incorporation of $^{15}NO_2^-$-derived ^{15}N into both $^{15}NO_2$-CLA and GS^{15} NO. In order to test this hypothesis, we utilized ^{15}N- and ^{18}O-labeled nitrite ($^{15}N^{18}O_2^-$) to differentiate between atoms coming from •NO autoxidation (^{14}N, ^{16}O) and those contributed exclusively by NO_2^-. This labeling strategy also reveals specifically symN_2O_3-derived atoms that yield mixed $^{14}N/^{18}O$ and $^{15}N/^{16}O$ isotopologues, such as $^{14}N^{16}O^{18}O$-containing •NO_2 (**2c,** Figure 5a). Importantly, the different •NO_2 and •NO isotopologues generated by symN_2O_3 homolysis can subsequently recombine with other •NO_2 and •NO molecules giving rise to further isotopic scrambling and the formation of new isotopologues such as $^{15}N^{18}O^{16}O_2^-$, $^{15}N^{16}O^{16}O$- and $^{14}N^{18}O^{18}O$-containing •NO_2, as well as $^{14}N^{18}O$- and $^{15}N^{16}O$-containing •NO.

$^{15}N^{18}O_2$-derived atoms were incorporated into NO_2-CLA primarily as mixed isotopologues at low $^{15}N^{18}O_2^-$ concentrations ($^{14}N^{18}O^{16}O$-CLA and $^{15}N^{18}O^{16}O$-CLA), but became more extensively incorporated to form $^{15}N^{18}O_2$-CLA when the concentration of $^{15}N^{18}O_2^-$ was increased (Figure 4b). Similar results were obtained when we added $^{15}N^{18}O_2^-$ to GSH in the presence of •NO and O_2, with lower $^{15}N^{18}O_2^-$ concentrations yielding mixed GSNO isotopologues and higher concentrations supporting more extensive formation of GS$^{15}N^{18}O$ (Figure 4c). While •NO concentration had a minor effect on the relative yields of NO_2-CLA isotopologues, $^{15}N^{18}O_2^-$ incorporation into GSNO was favored at higher •NO concentrations, consistent with a predominant role for N_2O_3-mediated nitrosation under these conditions (Supplementary Fig. 6) [3].

N_2O_3 participates in NO_2^--mediated nitration reactions

The preceding results indicated that NO_2^- incorporation into NO_2-CLA and GSNO involved symN_2O_3. To assess whether N_2O_3 formation is required for NO_2^- incorporation into NO_2-CLA, we evaluated direct CLA nitration by •NO_2 gas and $^{15}N^{18}O_2^-$ in the absence of •NO. While •NO_2 mediated substantial NO_2-CLA formation, only a minor fraction of the products incorporated $^{15}N^{18}O_2^-$-derived atoms and no mixed isotopologues were detected (Figure 5a-b). Comparison of the relative yields of NO_2^-- derived NO_2-CLA in the presence (Figure 2e-f) or absence of •NO (Figure 5b), indicated that the role of •NO in NO_2^--dependent nitration extends beyond •NO_2 formation. Additionally, we ruled out a potential role for NO_2^+ in CLA nitration under our experimental conditions by using nitronium tetrafluoroborate NO_2BF_4 as a nitrating agent (Supplementary Fig. 7). These results are consistent with previous reports indicating that NO_2^+ is an extremely short-lived species in aqueous solution due to preferential reaction with OH^- to generate NO^{3-} [28,29].

Next, we utilized nitrosonium tetrafluoroborate ($NOBF_4$) as a •NO-independent source of nitrosating equivalents (NO^+) in organic solvent to test the possibility that NO_2^--derived N_2O_3 formation supports the incorporation of NO_2^- atoms into NO_2-CLA. While NOBF4 failed to induce CLA nitration per se, the further addition of $^{14}NO_2^-$ led to substantial $^{14}NO_2$-CLA formation (Figure 5c). Also, addition of $^{15}N^{18}O_2^-$ to $NOBF_4$ resulted not only in $^{15}N^{18}O_2$-CLA generation but also yielded the mixed isotopologue $^{15}N^{16}O^{18}O$-CLA, consistent with symN_2O_3 formation upon NO_2^- nitrosation (Figure 5d). Further support for the formation of symN_2O_3 from the reaction between NO_2^-

and $NOBF_4$ was obtained by following 2,3-diaminonaphtalene (DAN) nitrosation to 2,3-naphtotriazole (NTA). We utilized DAN in lieu of GSH due to the poor solubility of GSH in non-aqueous solvents. As expected, $NOBF_4$ mediated only ^{14}NTA formation in the absence of $^{15}NO_2^-$ (Figure 5e). Addition of $^{15}NO_2^-$ to $NOBF_4$ significantly increased ^{15}NTA yields, consistent with the notion that NO_2^- nitrosation led to $symN_2O_3$ formation (Figure 5f). Figure 5g shows alternative mechanisms for $symN_2O_3$ formation from NO_2^-.

NO_2^--derived $symN_2O_3$ is generated during inflammation

To test whether $symN_2O_3$ formation occurs *in vivo*, we induced inflammation in mice by intraperitoneal (i.p.) injection of LPS, followed by i.p. administration of CLA (2.5 mg) +/− $^{15}N^{18}O_2^-$ 18 h later. This model caused an extensive influx of inflammatory monocytes and neutrophils which, together with a minor dendritic cell population, promoted increased generation of iNOS-derived secondary reactive species in the peritoneal cavity (Supplementary Fig. 8). Importantly, the doses of $^{15}N^{18}O_2^-$ utilized for these experiments (20 and 200 nmol) were well within the range of concentrations that are protective in animal models of ischemia and reperfusion injury [30]. Furthermore, analysis of NO_2^- levels at the time of peritoneal lavage showed that exogenously-added $^{15}N^{18}O_2^-$ represented less than 10 % of the total endogenous concentration of this anion (Supplementary Table 1). Notably, both $^{14}N^{16}O_2$-CLA and $^{15}N^{18}O_2^-$-derived isotopologues were detected (Figure 6a-c). The dose-dependent formation of $^{15}N^{18}O^{16}O$, $^{14}N^{18}O^{16}O$ and $^{15}N^{16}O^{16}O$-containing NO^2- CLA isotopologues recapitulated the *in vitro* responses (Figure 4b and S4c), indicating that biologically generated $^{\bullet}NO$ and $^{\bullet}NO_2$ promote $^{15}N^{18}O_2^-$ incorporation into $symN_2O_3$ *in vivo* (Figure 6b-c and e-f). The atomic composition of each individual species was unequivocally confirmed by high resolution hybrid FT-MS (Supplementary Fig. 9 and Supplementary Table 2). A drop in peritoneal pH during inflammation could potentially affect nitration by $symN_2O_3$. In this regard, inflammation results in a slight pH decrease in the peritoneal cavity, with values changing from 7.41 to 7.29 in humans, 7.32 to 7.19 in cats, and remaining unaltered in dogs (no data available for rodents) [31,32]. In this regard, we observed a decrease in the yield of *in vitro* CLA nitration resulting from $^{\bullet}NO$ autoxidation in the presence of $^{15}N^{18}O_2^-$ at pH values below 7.0. Importantly, the distribution of NO_2-CLA isotopologues was not affected across the pH interval, suggesting no direct effect of pH on $symN_2O_3$ formation (Supplementary Fig. 10). Finally, we recapitulated these results using the short half-life (less than 2 s) $^{\bullet}NO$ donor proli- NONOate, affirming that the decrease in NO_2-CLA formation observed at lower pH was not due to changes in the rate of $^{\bullet}NO$ release.

DISCUSSION

Nitrite, firmly established as a metastable physiologic $^{\bullet}NO$ reserve, is also a source of nitrosating and nitrating intermediates that expand the scope of mechanisms and secondary mediators that can transduce cell signaling events mediated by redox reactions [33,34]. In accordance with this concept, $^{15}NO_2^-$ addition to activated macrophages induced ^{15}NO-CLA formation in a dose-dependent manner. The relative contributions of different cell compartments to fatty acid nitration have not been characterized, as many of the reactive species involved in this process, -including both the substrate CLA and the resulting NO_2-

CLA, are readily diffusible and membrane permeable. However, the observed yields and kinetic profiles of CLA nitration by activated macrophages suggested that the free fatty acid, rather than esterified species, was the substrate for NO_2-CLA formation under the present conditions. Importantly, inhibition of $^{\bullet}NO$ synthesis abrogated both $^{14}NO_2$-CLA and $^{15}NO_2$-CLA generation, revealing an essential role for $^{\bullet}NO$ in CLA nitration by $^{15}NO_2^-$. While the acidification of NO_2^- (pK_a 3.46) in compartments such as the stomach, mitochondrial intermembrane space or phagolysosomes, favors the generation of HNO_2 and secondary species, current perspective holds that NO_2^--mediated nitration and nitrosation reactions at neutral pH is otherwise the consequence of metal catalysis [16,19-21,23,25]. Herein, we report the novel concept that NO_2^- participates in $^{\bullet}NO$ autoxidation-mediated nitration and nitrosation reactions at neutral pH in the absence of cellular constituents and adventitious metals.

The incorporation of ^{15}N into both NO_2-CLA and GSNO during $^{\bullet}NO$ autoxidation indicated that $^{15}NO_2^-$ not only generates a nitrating species, but also forms either $^{15\bullet}NO$ or a species capable of direct ^{15}N-nitroso transfer. A potential explanation involves the initial oxidation of $^{15}NO_2^-$ to $^{15\bullet}NO_2$, followed by reaction with $^{14\bullet}NO$ to generate $^{15}N^{14}N$-containing N_2O_3. The most commonly-cited structure for N_2O_3 entails an asymmetrical conformation with nitrosyl and nitryl moieties connected by a weak N-N bond [35]. However, homolytic scission of this bond would regenerate $^{14\bullet}NO$ and $^{15\bullet}NO_2$, and direct N_2O_3 reaction with a thiol would mediate ^{14}N-nitroso transfer via concerted nucleophilic substitution. These latter reactions did not explain the formation of $GS^{15}NO$ from $^{15}NO_2^-$. While asymN_2O_3 is the most stable candidate intermediate structure, alternative N_2O_3 conformations have been detected in low-temperature matrices and liquid xenon [36-38], including a symmetrical species in which two equivalent nitroso groups are connected to a central oxygen via identical N-O bonds. The stochastic cleavage of the internal N-O bonds in symN_2O_3 generated from $^{15\bullet}NO_2$ and $^{14\bullet}NO$, would lead to random distribution of the ^{15}N-atom. In other words, symmetrical $^{14}N,^{15}N$ N_2O_3 is equally able to generate $^{14\bullet}NO$ or $15^{\bullet}NO$, thus accounting for $^{15}NO_2^-$-derived $GS^{15}NO$ formation.

Symmetrical N_2O_3 is only marginally less stable than the asymmetrical isomer [37-41]. It has been predicted that symN_2O_3 represents a proportion of total N_2O_3 under physiological conditions, and symN_2O_3 has been proposed as an obligatory intermediate in the generation of asymN_2O_3 [5,42]. Herein, the aqueous neutral pH reactions of $^{15}N^{18}O_2^-$ yielded not only purely $^{\bullet}NO$ ($^{14}N/^{16}O$) and $^{15}N^{18}O_2^-$-derived products, but also mixed $^{14}N/^{18}O$ and $^{15}N/^{16}O$ isotopologues (Figure 4). This indicated that the reaction between NO_2^- and species generated during $^{\bullet}NO$ autoxidation entails more than a mere electron exchange and rather point at the formation of a covalent intermediate involving $^{\bullet}NO$- and NO_2^--derived atoms. Furthermore, the distribution of GSNO and NO_2-CLA isotopologues supported that NO_2^- is a precursor for symN_2O_3 formation during $^{\bullet}NO$ autoxidation. Consistent with the canonical mechanism for $^{\bullet}NO$ autoxidation (Reactions 1-4), lower O2 tensions and K4Fe(CN)6 supplementation decreased yields of both $^{\bullet}NO$- and $^{15}NO_2^-$-derived NO_2CLA and GSNO, indicating $^{\bullet}NO_2$ as an intermediate in these reactions [24,43]. It is possible that $^{\bullet}NO$ autoxidation does not yield “free” $^{\bullet}NO_2$, but rather produces an unidentified NOx intermediate capable of both oxidizing $K_4Fe(CN)_6$ and nitrosating thiols [18,44]. The present

report, showing NO_2-CLA formation during •NO autoxidation, implicates •NO_2 as the proximal nitrating species but does not exclude the possibility that symN_2O_3 could also directly mediate CLA nitration [45].

Two mechanisms can be envisaged by which NO_2^- gives rise to symN_2O_3; either NO_2^- oxidation to •NO_2 followed by reaction with •NO or a direct nucleophilic substitution (Figure 5g). Either mechanism is consistent with the observed dose-dependent increase in isotopic incorporation of $^{15}NO_2^-$ where net product yields are similar (Figures 2 and 3). The formation of $^{15}N^{18}O_2$-CLA (Figure 5a-b) indicated that ^{14}•NO_2 gas oxidizes $^{15}N^{18}O_2^-$ to ^{15}•$N^{18}O_2$ [46]. However, the lower relative yields of $^{15}N^{18}O_2$-CLA obtained using •$^{14}NO_2$ gas versus •$^{14}NO/O_2$ indicated that •NO promotes NO_2^- incorporation into NO_2-CLA to a greater extent than when electron self-exchange occurs between NO_2^- and •NO_2 gas. A role for nitrosodioxyl radical (ONOO•) generated during •NO autoxidation in NO_2^- oxidation to •NO_2 is unlikely, as this reaction is thermodynamically unfavorable (•NO_2/NO_2^- E° = +1.04 V vs. NHE and ONOO•/ONOO- E° = +0.511 V vs. NHE [46-49]). An additional mechanism for NO_2^- incorporation into N_2O_3 involves a substitution reaction in which a nucleophilic atom in NO_2^- attacks the nitroso moiety in •NO/O2-derived N_2O_3. The conformation of the resulting N_2O_3 could be either asymmetrical or symmetrical, depending on whether the nucleophilic attack is mediated by nitrogen or oxygen atoms, respectively.

To further assess the role of N_2O_3 in the formation of nitration and nitrosation products, we used $NOBF_4$ as a •NO-independent source of nitrosating equivalents. While this reaction system departs from biological conditions, it adds perspective to the concept of N_2O_3 generation occurring via NO_2^- nitrosation. No NO_2-CLA was formed from NOBF4 alone, however addition of $^{15}N^{18}O_2^-$ yielded not only $^{15}N^{18}O_2$-CLA but also the mixed $^{15}N^{16}O^{18}O$ isotopologue, supporting that •NO_2 was formed secondary to NO_2^- nitrosation (Figure 5d). Additionally, while $NOBF_4$ was sufficient to induce ^{14}NTA formation, $^{15}NO_2^-$ addition led to ^{15}NTA production, consistent with the formation of an intermediate species capable of ^{15}N-nitroso transfer. In aggregate, these results indicated that $^{15}NO_2^-$ nitrosation generates a symN_2O_3 intermediate that can mediate the incorporation of ^{15}N into both nitrated and nitrosated products.

Inflammatory responses are associated with increased production of reactive species capable of mediating oxidation, nitration and nitrosation reactions [50]. To test whether these species can induce symN_2O_3 formation from NO_2^- in a biological milieu, we analyzed CLA nitration products during acute inflammation in a murine model of peritonitis. There was significant CLA nitration induced by endogenously-generated •NO_2, as indicated by the detection of $^{14}N^{16}O$ NO_2-CLA in peritoneal lavage (Figure 6). Notably, the administration of $^{15}N^{18}O_2^-$ revealed dose-dependent generation of not only $^{15}N^{18}O^{18}O$-CLA, but also the scrambled isotopologues $^{15}N^{18}O^{16}O$-, $^{14}N^{18}O^{16}O$- and $^{15}N^{16}O^{16}O$-CLA. This indicated that endogenouslygenerated reactive species mediate NO_2^- incorporation into symN_2O_3 *in vivo*. Importantly, whereas different metal-dependent and -independent nitration mechanisms might be simultaneously operative *in vivo*, data from metal-free reaction systems indicated that NO_2^- -derived symN_2O_3 formation does not require either metal centers or additional cell-derived components.

The discovery that NO_2^- supports the generation of both electrophilic fatty acid nitroalkenes and nitrosothiols *in vivo* provides new perspective for understanding the broad array of cell signaling and physiological responses that can be instigated by NO_2^- [13,33]. The present *in vitro* and *in vivo* evidence also reveals a novel role for NO_2^- in the concerted generation of nitrating and nitrosating intermediates via the formation and stochastic homolysis of $symN_2O_3$.

ONLINE METHODS

Materials

9,11-Conjugated linoleic acid (CLA, 90%) was obtained from Nu-Check Prep, Inc (Elysian, MN, USA). $^{15}N^{16}O_2$ (98%) and $^{15}N^{18}O_2$ (^{15}N, 98%; ^{18}O, 90%) sodium nitrite were from Cambridge Isotope Laboratories (Andover, MA, USA). 1400W, deta-NONOate and mahma-NONOate (MNO) were from Cayman Chemical (Ann Arbor, MI, USA). $^{13}C_{18}$-nitro-oleic acid was synthesized in house [51]. Chemical characterization of the $^{13}C_{18}$-nitro-oleic acid batch utilized herein was not different from previously published reports [51]. All other chemicals were of analytical grade and were obtained from Sigma (St. Louis, MO, USA). Animals were housed in accordance with the Guide for the Care and Use of Laboratory Animals published by the US National Institutes of Health (NIH Publication No. 85-23, revised 1996). All procedures were approved by the University of Pittsburgh Institutional Animal Care and Use Committee (Approval # 14084265).

CLA nitration by RAW264.7 cells

Cells were maintained in DMEM (Mediatech, Manassas, VA, USA) plus 10 % fetal bovine serum (FBS, Gibco-Life Technologies, Waltham, MA, USA) at 37 °C, 95 % air and 5 % CO_2. Cells were treated with 50 μM CLA, 100 ng/mL LPS and 200 U/mL IFNγ, and incubated with or without 100 μM 1400W plus or minus 200 μM deta-NONOate in DMEM plus 1 % FBS. Media was collected at 24 h, spiked with internal standard (10 pmoles), and NO_2-CLA extracted using C18 SPE columns (Thermo Scientific, Waltham, MA, USA) as described previously [14].

Nitration and nitrosation reactions

CLA, 2,3-diaminonaphtalene (DAN) or glutathione (GSH), (20 μM) were incubated with MNO (25 μM for nitration and 2.5 μM for nitrosation reactions respectively) and NO_2^- (0 - 2 mM) in the presence or absence of $K_4Fe(CN)_6$ (1 mM) in 20 mM BisTris pH 7.0 containing 100 μM DTPA. Experiments using $NOBF_4$ were performed in acetonitrile to prevent reagent hydrolysis. Reactions were started by quick addition of a reaction mixture to 2 mL vials containing 10 μL of a 200x MNO stock solution. Vials were filled to capacity to eliminate headspace, sealed and immediately placed in an HPLC autosampler at 25 °C. Kinetic profiles were obtained by repeated injection of the reaction mixtures in a LCMS/MS system. For experiments in which Proli-NONOate was used, 10 μL of a 200x stock was added to sealed vials filled to capacity using a Hamilton syringe. Quantification of NO_2-CLA, S-nitrosoglutathione (GSNO) and 2,3-naphtotriazole (NTA) was performed using calibration curves prepared from either synthetic or commercially-available standards. ^{13}C-nitro-oleic acid, 1,4-piperazinediethanesulfonic acid (PIPES) and caffeine were utilized as

internal standards for NO_2-CLA, GSNO and NTA quantification respectively. Low-oxygen experiments were performed in a hypoxic chamber (COY Lab Products, Grass Lake, MI, USA).

CLA nitration with $^{\bullet}NO_2$ gas

CLA (20 μM) and $^{15}N^{18}O_2^-$ (200 μM, 2 mM) in 20 mM BisTris buffer pH 7.0 containing 100 μM DTPA were exposed to humidified $^{\bullet}NO_2$ gas (10.4 ±0.2 ppm in air, less than 0.1 ppm $^{\bullet}NO$) for 30 min at 160 mL/min under constant stirring in the dark. NO_2-CLA formation was measured by LC-MS/MS.

Peritoneal inflammation model

Male C57BL/6J mice, aged 10-12 weeks, were injected intraperitoneally with 20 μg LPS (6×10^4 endotoxin units) dissolved in a saline plus Freund's incomplete adjuvant (1:1) vehicle. Freund's incomplete adjuvant was utilized in conjunction with LPS to create an emulsion and induce localized, sustained inflammation in the peritoneum. This response relies on toll-like receptor 4 (TLR4) activation by LPS, an approach that was preferred over the more general and painful inflammation caused by the inactivated *M. tuberculosis* present in the complete adjuvant. Mice were rested overnight and subsequently treated with 2.5 mg CLA plus 0-200 nmol $Na^{15}N^{18}O_2^-$ in a phosphate buffered saline (PBS)/polyethylene glycol-400 vehicle 18 h post-LPS challenge. Mice were killed 1 h later and peritoneal lavage performed using PBS containing 2 mM EDTA. Lavagate was centrifuged and the cell-free supernatant extracted by C18 solid phase extraction (SPE) columns to enrich fatty acids and remove salts, followed by nitrated fatty acid purification with aminopropyl SPE columns. Briefly, C18 eluates were dried and resuspended in hexane:methyl tert-butyl ether:acetic acid (100:3:0.3) and loaded into hexane- equilibrated aminoproyl SPE columns. Non-polar complex lipids were removed with chloroform:isopropanol (2:1) followed by free fatty acid elution with diethyl ether:acetic acid (196:4). Nitrated fatty acids in the polar lipid fraction were measured by LC-MS/MS as described below.

Peritoneal NO_2^- measurement

Total NO_2^- levels were determined in peritoneal lavages by ozone-based I_3^- reductive chemiluminescence as described [52]. To differentiate exogenous ^{15}N- versus endogenous ^{14}N-containing nitrite, DAN diazotization to either ^{14}NTA or ^{15}NTA was determined by LC-MS/MS. Briefly, peritoneal lavagate dilutions were reacted with 30 μM DAN under acidic conditions for 10 min followed by alkalinization by sodium hydroxide addition to stop the reaction and LC-MS/MS analysis.

Analysis of peritoneal cell populations

Cell subpopulations in the peritoneal lavage were identified by flow cytometry analysis via staining with fluorochrome-conjugated antibodies against the following antigens: Ly-6G, MHC II, CD11c, F4/80, CD11b, CD86 (eBioscience). For iNOS expression analysis, cells were fixed and permeabilized with Fix/Perm Buffer (BD Biosciences) and stained with mouse anti-iNOS (Santa Cruz Biotechnology) and PE-anti-rabbit IgG (Jackson

ImmunoResearch Lab). Samples were acquired using a LSRII flow cytometer (BD) and analyzed with FlowJo software (TreeStar).

LC-MS/MS analysis

Nitrated fatty acid samples from *in vitro* experiments were resolved by C18 reverse-phase chromatography (Gemini 2 × 20 mm, 3 μm, Phenomenex, Torrance, CA) using 10 mM ammonium acetate/acetonitrile mobile phase system. Samples were loaded at 35 % acetonitrile at 0.75 mL/min, maintained for 0.2 min and the organic phase was increased to 90 % over 2 min. The column was then washed with 100 % acetonitrile for 1.2 min and reequilibrated at 35 % for an additional 0.8 min. Nitrated fatty acids extracted from cell media and peritoneal lavage were resolved with an analytical C18 Luna column (2 × 100 mm, 5 μm particle size; Phenomenex) at a 0.65 ml/min flow rate and an acetonitrile/water mobile phase system in the presence of 0.1 % acetic acid. Samples were loaded at 35 % acetonitrile/acetic acid for 1 min, followed by a linear increase in the organic phase to 90 % over 8 min. The column was then washed with 100 % acetonitrile/acetic acid for 3 min and re-equilibrated at 35 % for 3 min. Mass spectrometry analysis was performed using either an API 5000 or an API Qtrap 4000 (Applied Biosystems, Framingham, MA) in the negative ion mode using the following settings: source temperature 650 °C, curtain gas: 50, ionization spray voltage: -4500, GS1: 55, GS2: 50, declustering potential: −70 V, entrance potential: −4 V, collision energy: −35 V and collision cell exit potential: −5 V. The following MRM transitions were used for NO_2-CLA detection: $^{14}N^{16}O_2$ (324.2/46), $^{15}N^{16}O_2$ (325.2/47), $^{14}N^{16}O^{18}O$ (326.2/48), $^{15}N^{16}O^{18}O$ (327.2/49), $^{14}N^{18}O^{18}O$ (328.2/50), $^{15}N^{18}O^{18}O$ (329.2/51), and $^{13}C_{18}$ NO_2-OA (344.2/46). For GSNO measurements, samples were loaded in a Hypercarb column (2.1 × 100 mm, 5 μm, Thermo Scientific) at 5 % acetonitrile using the same mobile phase as above; organic phase percentage was maintained for 0.3 min and then increased to 70 % within 2.2 min. The column was washed with 100% acetonitrile for 0.7 min and then re-equilibrated for 0.7 min. MS analysis was performed in the positive ion mode at 550 °C, curtain gas 40, IS voltage 5500, GS1: 50, GS2: 50, DP: 40 V, EP: 9 V, CE: 13V and CXP: 9 V. For the internal standard, DP was 110 V, EP 10 V, CE 37 V and CXP 13 V. GSNO was detected using the following transitions: $^{14}N^{16}O$ (337.3/307.3), $^{15}N^{16}O$ (338.3/307.3), $^{14}N^{18}O$ (339.3/307.3), $^{15}N^{18}O$ (340.3/307.3) and PIPES (303.2/152.2). Finally for DAN nitrosation reactions, samples were loaded on a Gemini C18 column at 5 % acetonitrile/95 % 10 mM ammonium acetate. The organic phase was held constant for 0.3 min and then increased to 75 % over the next 2.3 min. The column was washed with 100 % organic phase for 0.7 min and then re-equilibrated for 0.7 min. NTA was measured in the positive ion mode at 650 °C, curtain gas: 40, IS voltage: 5500, GS1: 55, GS2: 50, DP: 70 V, EP: 5 V, CE: 35 V and CXP: 5 V. For the internal standard DP was set at 80 V, EP at 10 V and CE at 27 V. MRM transitions were: ^{14}NTA (170.1/115.1), ^{15}NTA (171.1/115.1) and caffeine (195.3/138.1).

High resolution mass spectrometric characterization of inflammation-derived NO_2-CLAisotopologues

Analytes of interest were characterized in both collision-induced dissociation (CID) and high collision energy dissociation (HCD) modes using an LTQ Velos Orbitrap (Velos Orbitrap, Thermo Scientific) equipped with a HESI II electrospray source. The following

parameters were used: source temperature 450 °C, capillary temperature 360 °C, sheath gas flow 20, auxiliary gas flow 15, sweep gas flow 3, Ion spray voltage 4 kV, S-lens RF level 41 (%). The instrument FT-mode was calibrated using the manufacturer's recommended calibration solution with the addition of malic acid as a low m/z calibration point in the negative ion mode. For MS/MS analysis of isotopologues, a window of 8 amu was selected for fragmentation, as isolation of individual isotopologues would not provide the necessary discrimination in the ion trap needed for these experiments. MS/MS analysis was performed at 60,000 resolution where discrimination of individual isotopologues (^{15}N, ^{13}C and ^{18}O) was achieved.

Statistical Analysis

Statistical analyses were performed using GraphPad Prism (La Jolla, CA. USA) version 6.05 by one-way or two-way analysis of variance (ANOVA) and Bonferroni multiple comparison test as indicated in the figure legends. P values below 0.05 were considered statistically significant.

Supplementary Material

Refer to Web version on PubMed Central for supplementary material.

Acknowledgements

This study was supported by NIH grants R01-HL058115, R01-HL64937, P30-DK072506, P01-HL103455 (BAF), R01-AT006822 (FJS) and AHA #14GRNT20170024 (FJS). We thank Drs. Mark T Gladwin, Jesus Tejero, Ana Maria Ferreira and Beatriz Alvarez for helpful discussions and Dr. Tim Sparwasser for expert assistance with flow cytometry experiments.

Abbreviations

1400W	N-[[3-(aminomethyl)phenyl]methyl]-ethanimidamide, dihydrochloride
BisTris	2,2-bis(hydroxymethyl)-2,2′,2″-nitrilotriethanol
$^{13}C_{18}$-nitro-oleic acid	10-nitro-octadec-9-enoic acid
CLA	(9Z,11E)-octadecadienoic acid
DAN	2,3-diaminonaphtalene
Deta-NONOate	2,2′-(Hydroxynitrosohydrazino)bis-ethanamine
DTPA	diethylene-triaminepentaacetic acid
EDTA	ethylenediaminetetraacetic acid
GSNO	S-nitroso-L-glutathione
iNOS	inducible nitric oxide synthase
LC-MS/MS	high-performance liquid chromatography-electrospray ionization tandem mass spectrometry

LPS	lipopolysaccharyde
MNO	mahma-NONOate, (Z)-1-[N-methyl-N-[6-(N-methylammoniohexyl)amino]]diazen-1-ium-1,2-diolate
NOS	nitric oxide synthase
NO_2-CLA	conjugated nitro-linoleic acid, mixture of positional isomers of 9- and 12-nitrooctadeca-9,11-dienoic acid
$^{\bullet}NO_2$	nitrogen dioxide
$^{\bullet}NO$	nitrogen monoxide
$NOBF_4$	nitrosonium tetrafluoroborate
NO_2BF_4	nitronium tetrafluoroborate
HNO_2	nitrous acid
NTA	2,3-naphtotriazole
PIPES	1,4-piperazinediethanesulfonic acid
Proli-NONOate	1-[(2-carboxylato)pyrrolidin-1-yl]diazen-1-ium-1,2-diolate
SPE	solid phase extraction
TLR4	toll-like receptor 4

REFERENCES

1. Maron BA, Tang SS, Loscalzo J. S-nitrosothiols and the S-nitrosoproteome of the cardiovascular system. Antioxid Redox Signal. 2013; 18:270–287. [PubMed: 22770551]
2. Bosworth CA, Toledo JC Jr. Zmijewski JW, Li Q, Lancaster JR Jr. Dinitrosyliron complexes and the mechanism(s) of cellular protein nitrosothiol formation from nitric oxide. Proc Natl Acad Sci U S A. 2009; 106:4671–4676. [PubMed: 19261856]
3. Lancaster JR Jr. Protein cysteine thiol nitrosation: maker or marker of reactive nitrogen species-induced nonerythroid cellular signaling? Nitric Oxide. 2008; 19:68–72. [PubMed: 18503780]
4. Moller MN, et al. Membrane “lens” effect: focusing the formation of reactive nitrogen oxides from the *NO/O2 reaction. Chem Res Toxicol. 2007; 20:709–714. [PubMed: 17388608]
5. Nedospasov AA. Is N2O3 the main nitrosating intermediate in aerated nitric oxide (NO) solutions in vivo? If so, where, when, and which one? J Biochem Mol Toxicol. 2002; 16:109–120. [PubMed: 12112710]
6. Broniowska KA, Keszler A, Basu S, Kim-Shapiro DB, Hogg N. Cytochrome c-mediated formation of S-nitrosothiol in cells. Biochem J. 2012; 442:191–197. [PubMed: 22070099]
7. Foster MW, Hess DT, Stamler JS. Protein S-nitrosylation in health and disease: a current perspective. Trends Mol Med. 2009; 15:391–404. [PubMed: 19726230]
8. Foster MW, et al. Proteomic characterization of the cellular response to nitrosative stress mediated by s-nitrosoglutathione reductase inhibition. J Proteome Res. 2012; 11:2480–2491. [PubMed: 22390303]
9. Souza JM, Peluffo G, Radi R. Protein tyrosine nitration--functional alteration or just a biomarker? Free Radic Biol Med. 2008; 45:357–366. [PubMed: 18460345]
10. Akaike T, Nishida M, Fujii S. Regulation of redox signalling by an electrophilic cyclic nucleotide. J Biochem. 2013; 153:131–138. [PubMed: 23248242]

11. Delmastro-Greenwood M, Freeman BA, Wendell SG. Redox-dependent anti-inflammatory signaling actions of unsaturated Fatty acids. Annu Rev Physiol. 2014; 76:79–105. [PubMed: 24161076]
12. Schopfer FJ, Cipollina C, Freeman BA. Formation and signaling actions of electrophilic lipids. Chem Rev. 2011; 111:5997–6021. [PubMed: 21928855]
13. Bonacci G, et al. Conjugated linoleic acid is a preferential substrate for fatty acid nitration. J Biol Chem. 2012; 287:44071–44082. [PubMed: 23144452]
14. Salvatore SR, et al. Characterization and quantification of endogenous fatty acid nitroalkene metabolites in human urine. J Lipid Res. 2013; 54:1998–2009. [PubMed: 23620137]
15. Charles RL, et al. Protection from hypertension in mice by the Mediterranean diet is mediated by nitro fatty acid inhibition of soluble epoxide hydrolase. Proc Natl Acad Sci U S A. 2014; 111:8167–8172. [PubMed: 24843165]
16. Lundberg JO, Weitzberg E. Biology of nitrogen oxides in the gastrointestinal tract. Gut. 2013; 62:616–629. [PubMed: 22267589]
17. Goldstein S, Czapski G. Kinetics of Nitric-Oxide Autoxidation in Aqueous-Solution in the Absence and Presence of Various Reductants - the Nature of the Oxidizing Intermediates. J Am Chem Soc. 1995; 117:12078–12084.
18. Wink DA, Darbyshire JF, Nims RW, Saavedra JE, Ford PC. Reactions of the bioregulatory agent nitric oxide in oxygenated aqueous media: determination of the kinetics for oxidation and nitrosation by intermediates generated in the NO/O2 reaction. Chem Res Toxicol. 1993; 6:23–27. [PubMed: 8448345]
19. van Faassen EE, et al. Nitrite as regulator of hypoxic signaling in mammalian physiology. Med Res Rev. 2009; 29:683–741. [PubMed: 19219851]
20. van der Vliet A, Eiserich JP, Halliwell B, Cross CE. Formation of reactive nitrogen species during peroxidase-catalyzed oxidation of nitrite. A potential additional mechanism of nitric oxide-dependent toxicity. J Biol Chem. 1997; 272:7617–7625. [PubMed: 9065416]
21. Ford PC. Reactions of NO and nitrite with heme models and proteins. Inorg Chem. 2010; 49:6226–6239. [PubMed: 20666383]
22. Castro L, Eiserich JP, Sweeney S, Radi R, Freeman BA. Cytochrome c: a catalyst and target of nitrite-hydrogen peroxide-dependent protein nitration. Arch Biochem Biophys. 2004; 421:99–107. [PubMed: 14678790]
23. d'Ischia M, Napolitano A, Manini P, Panzella L. Secondary targets of nitrite-derived reactive nitrogen species: nitrosation/nitration pathways, antioxidant defense mechanisms and toxicological implications. Chem Res Toxicol. 2011; 24:2071–2092. [PubMed: 21923154]
24. Goldstein S, Czapski G. Mechanism of the Nitrosation of Thiols and Amines by Oxygenated•NO Solutions: the Nature of the Nitrosating Intermediates. J Am Chem Soc. 1996; 118:3419–3425.
25. Basu S, et al. Catalytic generation of N2O3 by the concerted nitrite reductase and anhydrase activity of hemoglobin. Nat Chem Biol. 2007; 3:785–794. [PubMed: 17982448]
26. Fernandez BO, Ford PC. Nitrite catalyzes ferriheme protein reductive nitrosylation. J Am Chem Soc. 2003; 125:10510–10511. [PubMed: 12940720]
27. Tejero J, et al. Low NO concentration dependence of reductive nitrosylation reaction of hemoglobin. J Biol Chem. 2012; 287:18262–18274. [PubMed: 22493289]
28. Beckman JS, et al. Kinetics of superoxide dismutase- and iron-catalyzed nitration of phenolics by peroxynitrite. Arch Biochem Biophys. 1992; 298:438–445. [PubMed: 1416975]
29. Ischiropoulos H, et al. Peroxynitrite-mediated tyrosine nitration catalyzed by superoxide dismutase. Arch Biochem Biophys. 1992; 298:431–437. [PubMed: 1416974]
30. Duranski MR, et al. Cytoprotective effects of nitrite during in vivo ischemia-reperfusion of the heart and liver. J Clin Invest. 2005; 115:1232–1240. [PubMed: 15841216]
31. Bonczynski JJ, Ludwig LL, Barton LJ, Loar A, Peterson ME. Comparison of peritoneal fluid and peripheral blood pH, bicarbonate, glucose, and lactate concentration as a diagnostic tool for septic peritonitis in dogs and cats. Vet Surg. 2003; 32:161–166. [PubMed: 12692761]
32. Sennesael JJ, De Smedt GC, Van der Niepen P, Verbeelen DL. The impact of peritonitis on peritoneal and systemic acid-base status of patients on continuous ambulatory peritoneal dialysis. Perit Dial Int. 1994; 14:61–65. [PubMed: 8312417]

33. Vitturi DA, Patel RP. Current perspectives and challenges in understanding the role of nitrite as an integral player in nitric oxide biology and therapy. Free Radic Biol Med. 2011; 51:805–812. [PubMed: 21683783]
34. Kansanen E, Jyrkkanen HK, Levonen AL. Activation of stress signaling pathways by electrophilic oxidized and nitrated lipids. Free Radic Biol Med. 2012; 52:973–982. [PubMed: 22198184]
35. Horakh J, Borrmann H, Simon A. Phase-Relationships in the N2O3/N2O4 System and Crystal-Structures of N2O3. Chem Eur J. 1995; 1:389–393.
36. Fateley WG, Bent HA, Crawford B. Infrared Spectra of the Frozen Oxides of Nitrogen. J Chem Phys. 1959; 31:204–217.
37. Holland RF, Maier WB. Infrared absorption spectra of nitrogen oxides in liquid xenon. Isomerization of N2O3 a). J Chem Phys. 1983; 78:2928–2941.
38. Varetti EL, Pimentel GC. Isomeric Forms of Dinitrogen Trioxide in a Nitrogen Matrix. J Chem Phys. 1971; 55:3813–3821.
39. Shaw AW, Vosper AJ. Dinitrogen trioxide. Part IX. Stability of dinitrogen trioxide in solution. J Chem Soc A. 1971:1592.
40. Jubert AH, Varetti EL, Villar HO, Castro EA. A theoretical study of the relative stability of the isomeric forms of N2O3. Theor Chim Acta. 1984; 64:313–316.
41. Sun Z, Liu YD, Lv CL, Zhong RG. Theoretical investigation of the isomerization of N2O3 and the N-nitrosation of dimethylamine by asym-N2O3, sym-N2O3, and trans–cis N2O3 isomers. J Mol Struct (Theochem). 2009; 908:107–113.
42. Zakharov II, Zakharova OI. Nitrosonium Nitrite Isomer of N2O3: Quantum-Chemical Data. J Struct Chem. 2009; 50:212–218.
43. Pryor WA, Lightsey JW, Church DF. Reaction of nitrogen dioxide with alkenes and polyunsaturated fatty acids: addition and hydrogen-abstraction mechanisms. J Am Chem Soc. 1982; 104:6685–6692.
44. Wink DA, et al. Reaction kinetics for nitrosation of cysteine and glutathione in aerobic nitric oxide solutions at neutral pH. Insights into the fate and physiological effects of intermediates generated in the NO/O2 reaction. Chem Res Toxicol. 1994; 7:519–525. [PubMed: 7981416]
45. Wink DA, Ford PC. Nitric Oxide Reactions Important to Biological Systems: A Survey of Some Kinetics Investigations. Methods. 1995; 7:14–20.
46. Huie RE. The reaction kinetics of NO2(.). Toxicology. 1994; 89:193–216. [PubMed: 8023329]
47. Galliker B, Kissner R, Nauser T, Koppenol WH. Intermediates in the autoxidation of nitrogen monoxide. Chemistry. 2009; 15:6161–6168. [PubMed: 19437472]
48. Amatore C, et al. Characterization of the electrochemical oxidation of peroxynitrite: Relevance to oxidative stress bursts measured at the single cell level. Chem Eur J. 2001; 7:4171–4179. [PubMed: 11686596]
49. Koppenol WH. Nitrosation, thiols, and hemoglobin: energetics and kinetics. Inorg Chem. 2012; 51:5637–5641. [PubMed: 22554003]
50. Pacher P, Beckman JS, Liaudet L. Nitric oxide and peroxynitrite in health and disease. Physiol Rev. 2007; 87:315–424. [PubMed: 17237348]
51. Woodcock SR, Bonacci G, Gelhaus SL, Schopfer FJ. Nitrated fatty acids: synthesis and measurement. Free Radic Biol Med. 2013; 59:14–26. [PubMed: 23200809]
52. Lang JD Jr. et al. Inhaled NO accelerates restoration of liver function in adults following orthotopic liver transplantation. J Clin Invest. 2007; 117:2583–2591. [PubMed: 17717604]

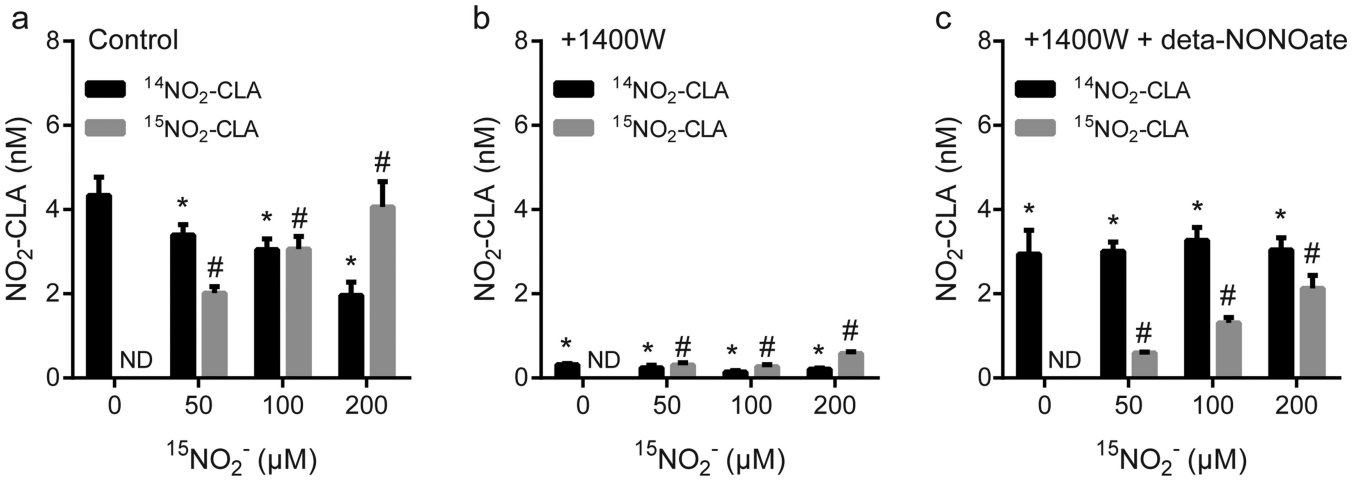

Figure 1. $^{15}NO_2^-$ incorporation into NO_2-CLA is dependent on $^{\bullet}NO$ production by activated RAW264.7 cells

a, CLA (50 μM) nitration by RAW264.7 cells activated with LPS and IFNγ for 24 h in the presence or absence of $^{15}NO_2^-$. Under these conditions, all $^{14\bullet}NO_2$ and $^{14}NO_2^-$ is derived from endogenous $^{14\bullet}NO$. *, # $p<0.0001$ versus 0 μM $^{15}NO_2^-$ for $^{14}NO_2$-CLA and $^{15}NO_2$-CLA respectively. **b**, NO_2-CLA formation by activated RAW264.7 cells in the presence of 1400W (100 μM). *, # $p<0.0001$ versus corresponding non-1400W treatments (in panel a) for $^{14}NO_2$-CLA and $^{15}NO_2$-CLA respectively. **c**, CLA nitration by 1400W-treated activated cells in the presence of deta-NONOate (200 μM). *,# $p < 0.0001$ versus corresponding 1400W alone treatment (in panel b). For all panels, data are mean ± SD (n=4) and two-way ANOVA plus Bonferroni's multiple comparison were used to test statistical significance.

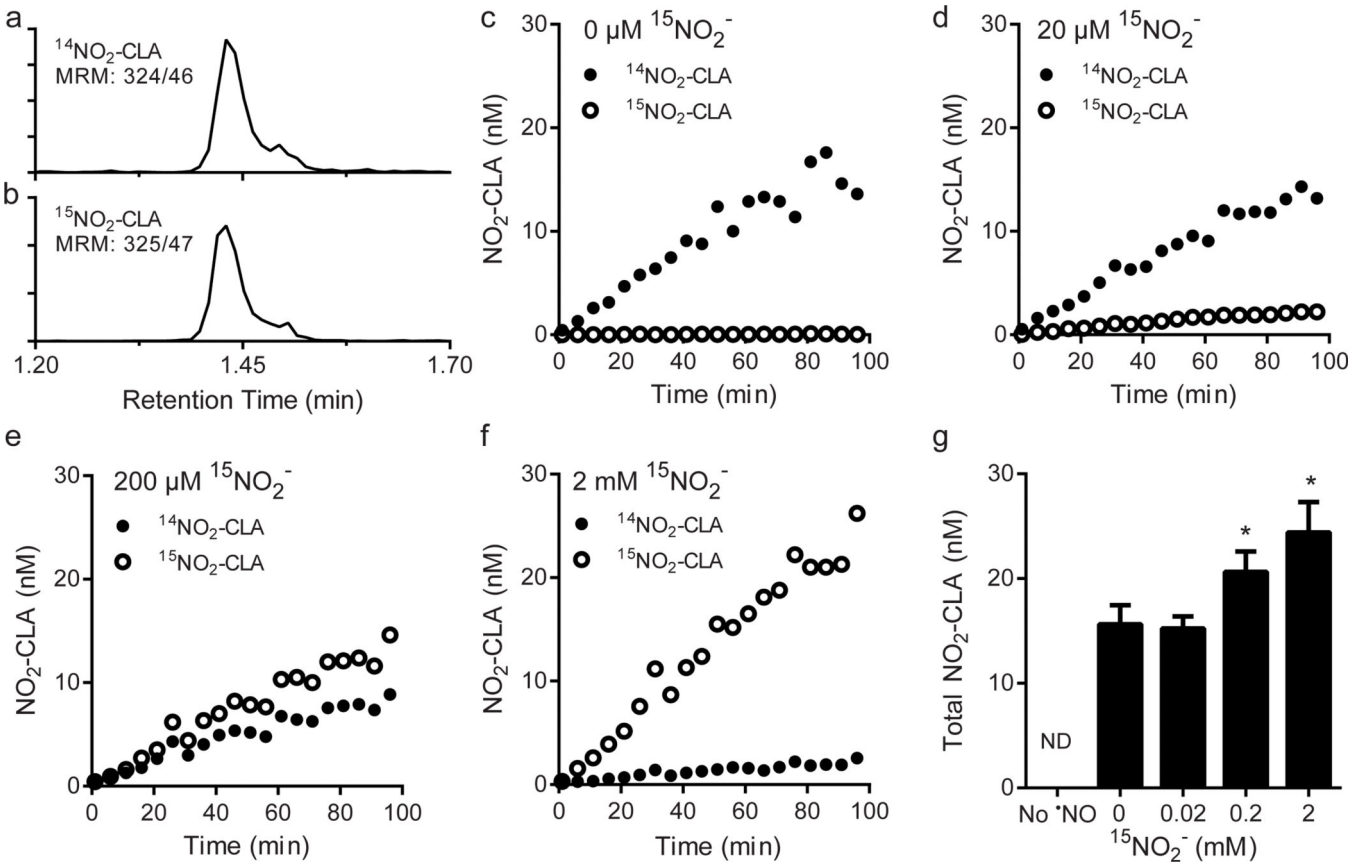

Figure 2. $^{15}NO_2^-$ participates in CLA nitration in the absence of cellular components

Representative LCMS/MS traces for $^{14}NO_2$-CLA (**a**) and $^{15}NO_2$-CLA (**b**) detection. **c-f,** Kinetic traces of $^{14}NO_2$-CLA and $^{15}NO_2$-CLA formation from 25 μM MNO and 20 μM CLA in the absence (**c**) or presence of 20 μM (**d**), 200 μM (**e**) and 2 mM (**f**) $^{15}NO_2^-$. Data are representative traces generated by combining time-staggered replicate reactions (n=4). **g**, Total yields of NO -CLA formation versus $^{15}NO_2^-$ concentration. Data are mean ± SD (n=4), * $p < 0.05$ versus 0 mM $^{15}NO_2^-$ as determined by one way ANOVA and Bonferroni's multiple comparison test. No NO -CLA formation was detected from 2 mM $^{15}NO_2^-$ in the absence of MNO.

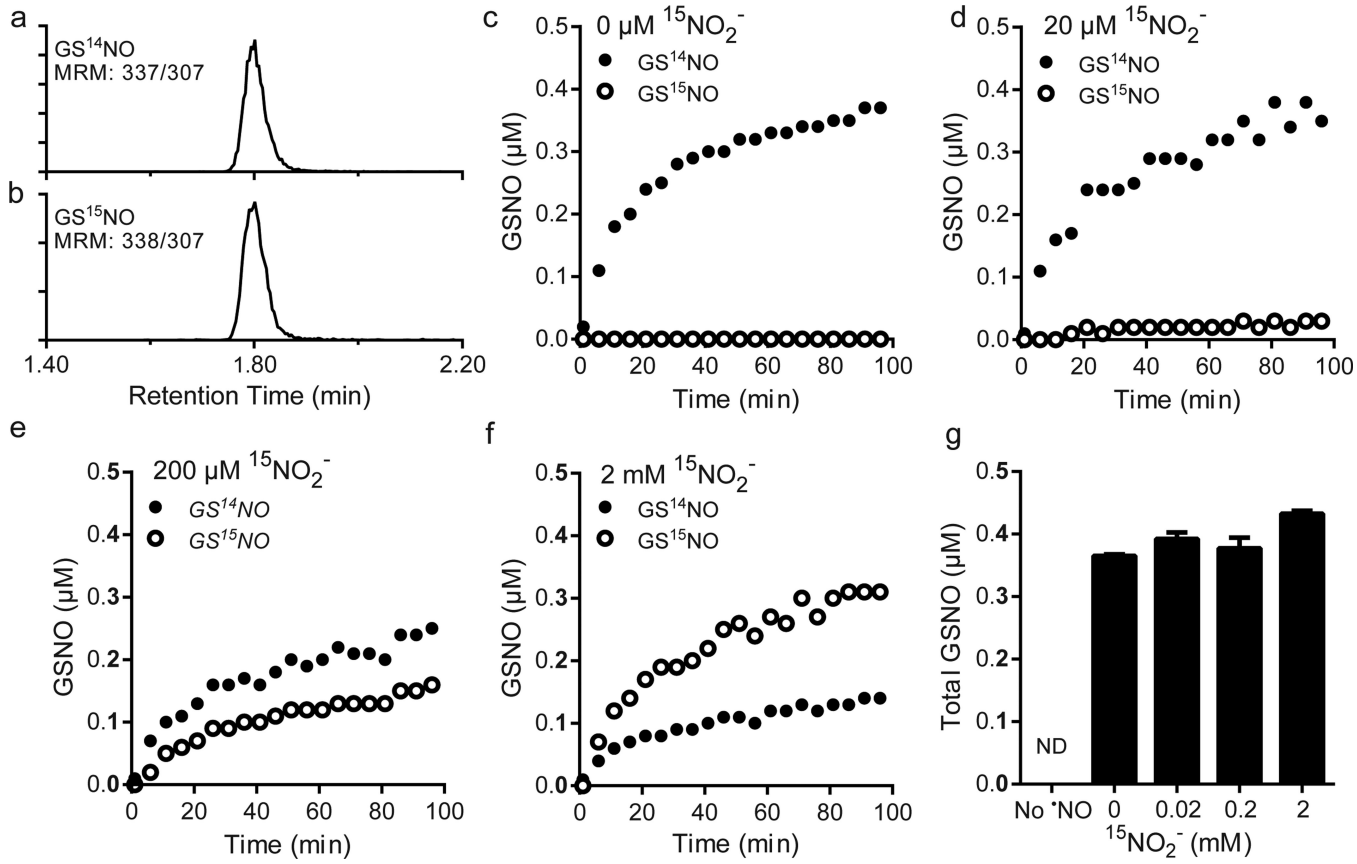

Figure 3. $^{15}NO_2^-$ mediates glutathione nitrosation in the presence of •NO

a-b, Representative LCMS/MS traces for $GS^{14}NO$ (a) and $GS^{15}NO$ (b) formation. **c-f**, Traces showing $GS^{14}NO$ and $GS^{15}NO$ formation from 2.5 μM MNO and 20 μM GSH in the absence (**c**) or presence of 20 μM (**d**), 200 μM (**e**) and 2 mM (**f**) $^{15}NO_2^-$. Traces are representative and reflect time-staggered replicate reactions (n=4). **g**, Total GSNO yields versus $^{15}NO_2^-$ concentration. Data are mean ± SD (n=4), no statistical differences were found as determined by one way ANOVA. No GSNO was formed from 2 mM $^{15}NO_2^-$ in the absence of MNO.

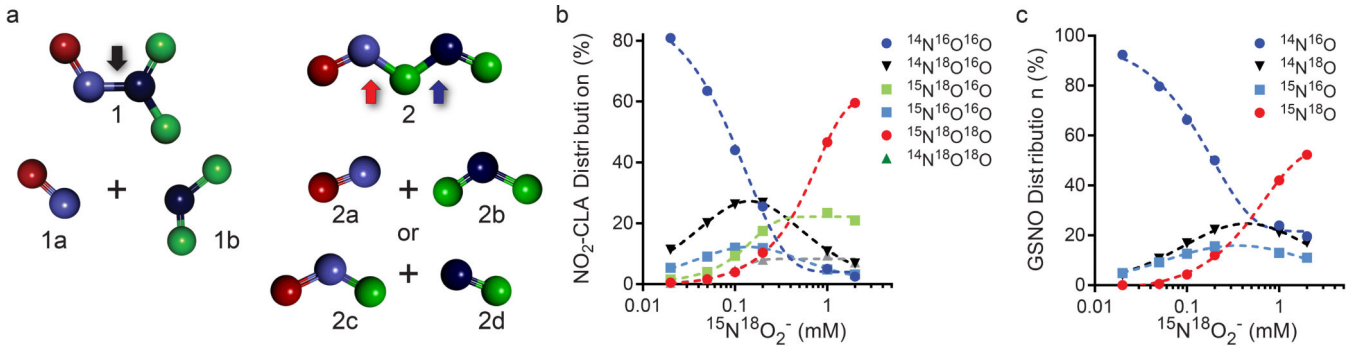

Figure 4. NO_2^- incorporation into NO_2-CLA and GSNO is associated with symN_2O_3 formation

a, Scheme illustrating the asymmetrical (**1**) and symmetrical (**2**) conformations of N_2O_3. Arrows indicate alternative bond cleavage patterns. Whereas asymN_2O_3 homolysis produces a unique set of products (1a, 1b), alternative cleavage of the O-N-O bonds in symN_2O_3 can be evidenced by isotopic labeling (blue and red represent ^{14}N and ^{16}O respectively, dark blue and green are ^{15}N and ^{18}O). **b**, Distribution of NO_2-CLA isotopologues versus $^{15}N^{18}O_2^-$ concentration in the presence of 25 μM MNO and 20 μM CLA. **c**, Isotopic GSNO distribution versus $^{15}N^{18}O_2^-$ in the presence of 2.5 μM MNO and 20 μM GSH. Data for panels b and c are mean ± SD (n=4). Error bars are not distinguishable as they overlap with data points.

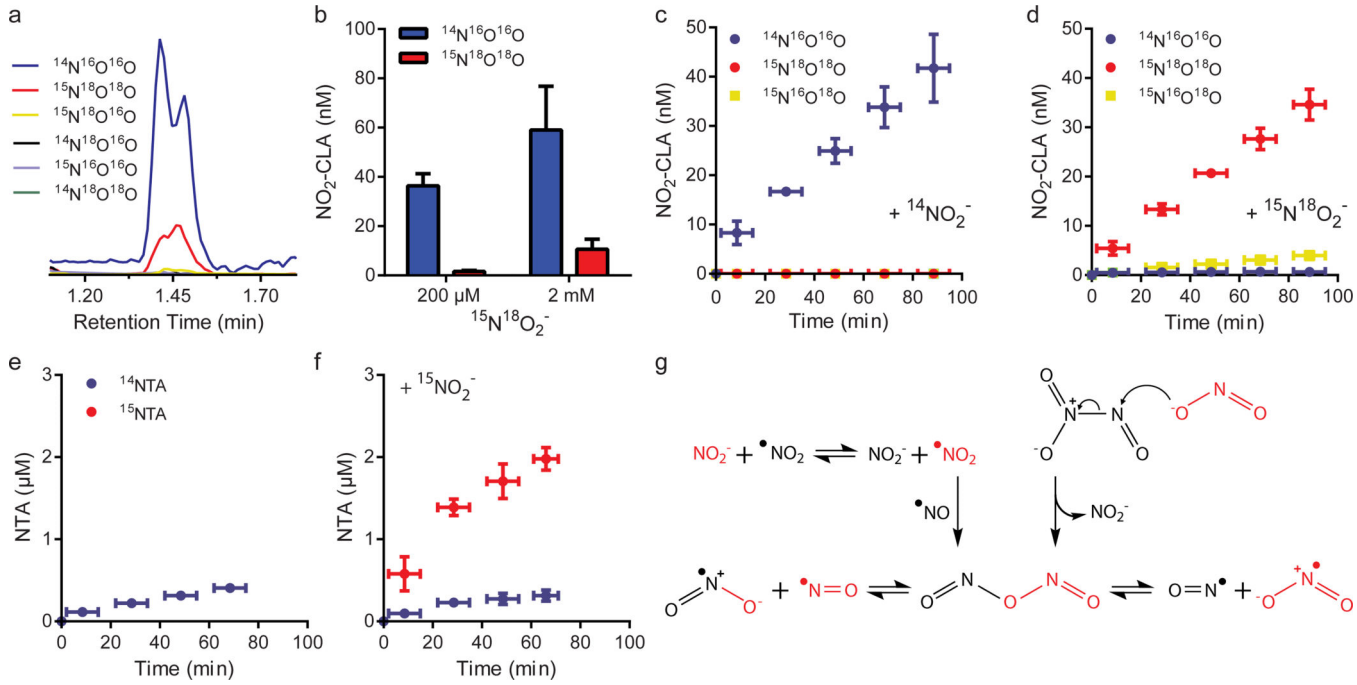

Figure 5. NO_2^- incorporation into nitrating and nitrosating equivalents requires reaction with $^{\bullet}$NO-derived species

a, LC-MS/MS trace showing the formation of $^{14}NO_2$-CLA and $^{15}N^{18}O_2$-CLA from CLA (20 μM) nitration by pure $^{\bullet}$NO gas in the presence of 2 mM $^{15}N^{18}O_2^-$. **b,** NO_2-CLA yields obtained from CLA nitration by $^{\bullet}$NO gas and $^{15}N^{18}O_2^-$. Data are means ± SD (n=3). **c-d,** NO_2-CLA formation from the reaction between 50 μM NOBF and either $^{14}NO_2^-$ (c) or $^{15}N^{18}O_2^-$ (d) in acetonitrile. Data are mean ± SD (n=4), with no NO_2-CLA formation observed in the absence of nitrite. **e-f,** NTA formation from the reaction between 20 μM DAN and 50 μM $NOBF_4$ in the absence (e) or presence (f) of 20 μM $^{15}NO_2^-$ $_2$in acetonitrile. Data are means ± SD (n=4). **g,** Proposed mechanisms for NO_2^- incorporation into nitrating and nitrosating species via $symN_2O_3$ formation.

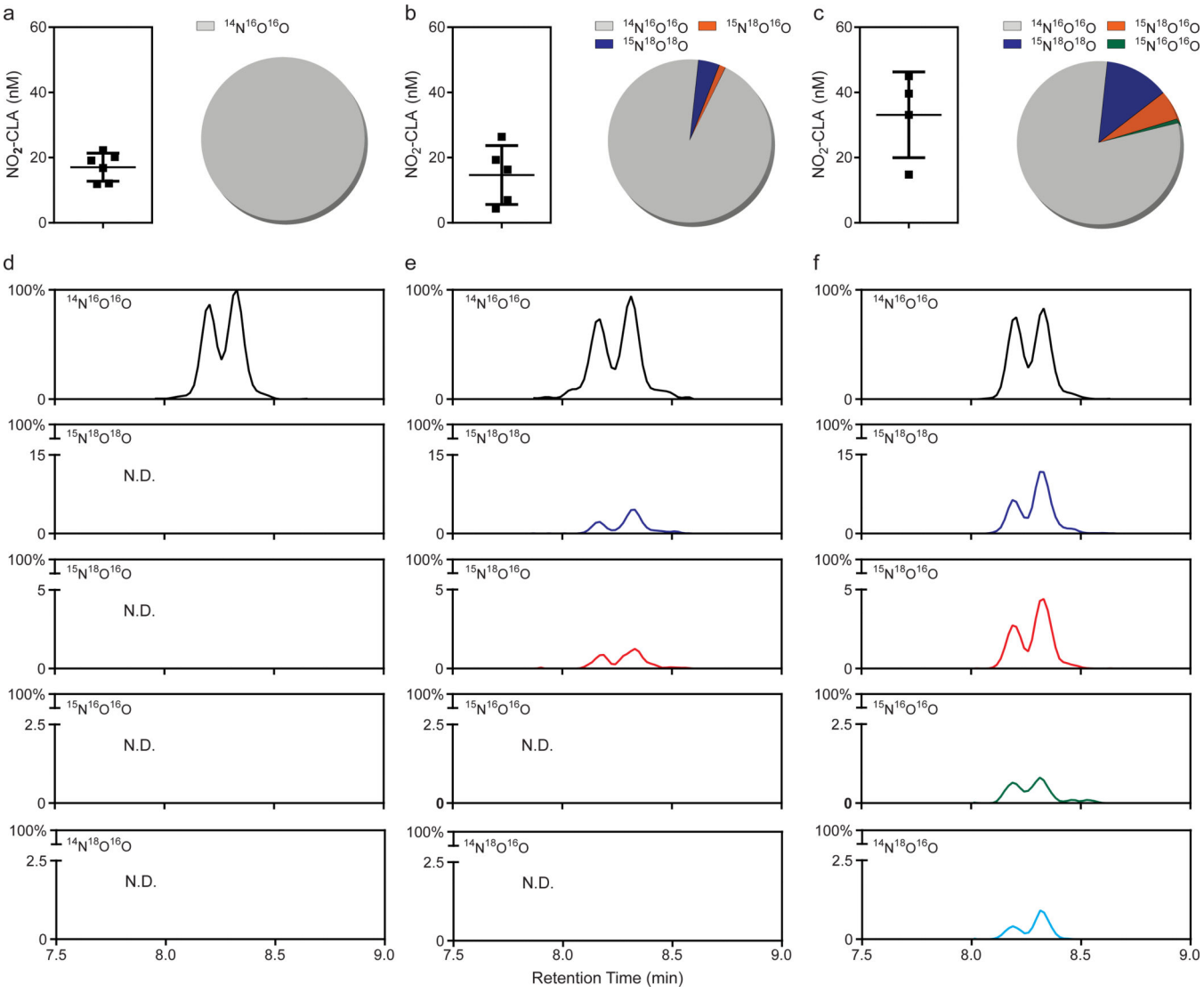

Figure 6. Inflammatory conditions promote NO_2^--dependent $symN_2O_3$ generation *in vivo*

a-c, Total concentrations and relative isotopic distributions of NO_2-CLA generated during peritoneal inflammation. Points represent measurements from individual animals with mean ± SD indicated by the lines. Mice were injected i.p. with 20 μg LPS and 18 h later received a second injection containing 2.5 mg CLA plus 0 (a), 20 (b) or 200 (c) nmol $^{15}N^{18}O_2^-$. **d-f,** Representative LC-MS/MS traces of NO_2-CLA isotopologue formation after administration of 0 (d), 20 (e) and 200 (f) nmol $^{15}N^{18}O_2^-$. $^{14}N^{18}O^{16}O$-containing NO_2-CLA levels were <0.5% of total and were not included in the isotopic distributions (a-c), $^{14}N^{18}O^{18}O$-containing NO_2-CLA was not detected.